Current Applied Physics 10 (2010) 60–63

Contents lists available at ScienceDirect

Current Applied Physics

journal homepage: www.elsevier.com/locate/cap

Structural, Raman, and photoluminescence characteristics of ZnO nanowires coated with Al-doped ZnO shell layers

Hyoun Woo Kim *, Mesfin Abayneh Kebede, Hyo Sung Kim

Division of Materials Science and Engineering, Inha University, Incheon 402-751, Republic of Korea

ARTICLE INFO

Article history:
Received 28 December 2008
Received in revised form 13 April 2009
Accepted 14 April 2009
Available online 3 May 2009

PACS:
81.07.−b
81.05.Dz
61.46.Km
68.37.Hk
68.37.Lp
78.55.Et

Keywords:
Nanowires
ZnO
Al-doped ZnO
Sputtering

ABSTRACT

Al-doped ZnO (AZO) shell layers were coated on core ZnO nanowires to fabricate ZnO/AZO core–shell nanowires. The energy-dispersive X-ray spectra confirmed the presence of Al element in the shell layers, and the lattice resolved transmission electron microscopy image revealed that these layers corresponded to the hexagonal ZnO structure. The X-ray diffraction pattern exhibited a shift of the ZnO peaks, suggesting the substitutive incorporation of Al into the ZnO lattice. The A_1(LO) mode line in the Raman spectra was enhanced by the AZO coating. In the photoluminescence measurements, the AZO coating enhanced the intensity ratio of the UV to green emission.

1. Introduction

As a group II–VI semiconductor material, zinc oxide (ZnO) has attracted a great deal of attention from scientists and technologists across the globe, because of its versatile and remarkable physical, optical and electronic properties. ZnO is an n-type oxide semiconductor material with a wide bandgap energy of 3.37 eV and high exciton binding energy of 60 meV and, hence, it has assumed great importance due to its intriguing and multi-optical functions [1–4].

Doped ZnO nanostructures have attracted much interest owing to their potential in nanodevice fabrication [5]. Aluminum (Al) is a widely used group III dopant, efficiently forming n-type ZnO. Additionally, Al-doped ZnO (AZO) films are useful materials for a variety of applications, including gas sensors [6], solar cells [7], optoelectronic devices [8], and flat panel displays [9].

In this paper, we report the preparation of ZnO/AZO core–shell nanowires. In order to fabricate nanowire-based devices with a p–n junction in the radial direction for future applications, it is necessary to develop a technique to deposit n-type AZO shell layers on core ZnO nanowires [10]. Furthermore, AZO shell layers can be used not only for the protection of the core ZnO nanowires from contamination or oxidation, but also to add a variety of functions. We conducted a comparative investigation of the samples before and after the AZO coating, in regard to their structural, Raman, and photoluminescence (PL) characteristics. To the best of our knowledge, this is first report on the coating of AZO layers on ZnO nanostructures.

2. Experimental

First, we synthesized ZnO nanowires by heating the Zn powders in a vertical tubular furnace [11], in which the Zn powders and Au-coated Si substrates were placed on the lower and upper holders in the center of the quartz tube, respectively. The gas flow rate of nitrogen (N_2) was 1.5 standard liters per min (slm). The substrate temperature was maintained at 900 °C for 1 h.

Subsequently, we carried out AZO coating experiments on the as-grown ZnO samples by using the rf sputtering technique [12]. AZO layers were deposited by rf sputtering at a pressure of

* Corresponding author.
E-mail address: hwkim@inha.ac.kr (H.W. Kim).

1567-1739/$ - see front matter © 2009 Elsevier B.V. All rights reserved.
doi:10.1016/j.cap.2009.04.012

0.02 Torr in an Ar ambient. The AZO target (ZnO: 97 wt.% and Al: 3 wt.%) was supplied by Taewon Scientific Co. Ltd., Korea. The rf power for the AZO target was set to 150 W. While the substrate temperature was fixed at 25 °C, the sputtering time was varied in the range of 1–3 min. The thicknesses of AZO layers sputtered for 1, 2, and 3 min are estimated to be about 10, 20, and 30 nm, respectively.

The structural properties were characterized by X-ray diffraction (XRD) (Philips X'pert MRD diffractometer with CuKα_1 radiation), field emission scanning electron microscopy (FE-SEM) (Hitachi, S-4200), transmission electron microscopy (TEM) (Philips, CM-200), and energy dispersive X-ray spectroscopy (EDX). Micro-Raman spectra were taken on a Renishow Ramoscope equipped with a He–Ne laser (λ = 633 nm). PL spectra were measured at room temperature following excitation with a He–Cd laser (λ = 325 nm, 55 mW). Both the Raman and PL measurements were done at room temperature.

3. Results and discussion

Fig. 1a shows a typical SEM image of the AZO-coated products, confirming their one-dimensional (1D) structure. Fig. 1b shows a

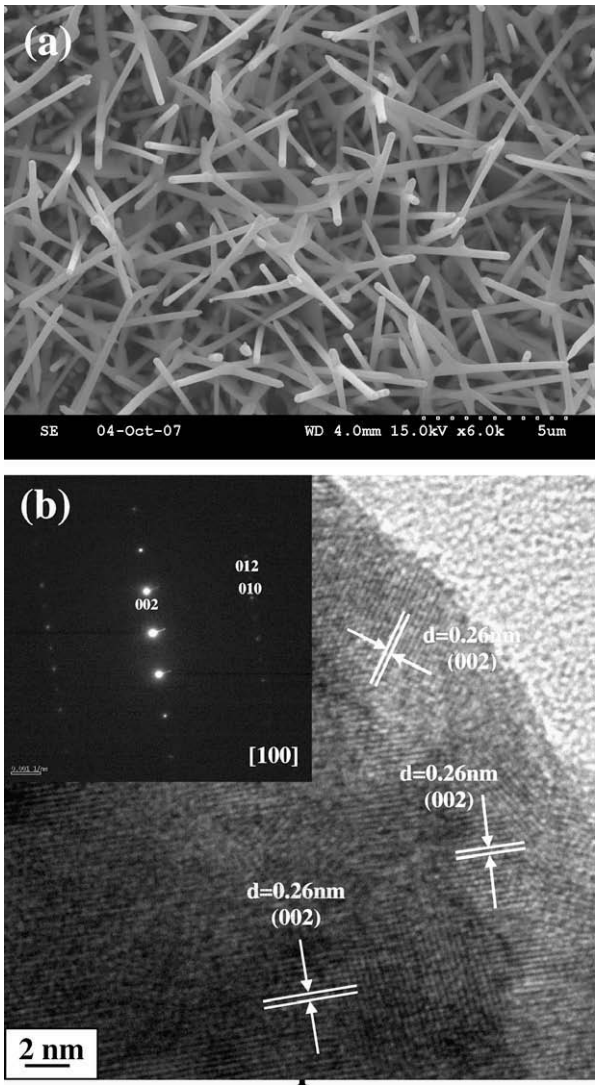

Fig. 1. (a) SEM image of the AZO-coated products. (b) TEM image of a AZO-coated ZnO nanowire. The inset shows the corresponding SAED pattern.

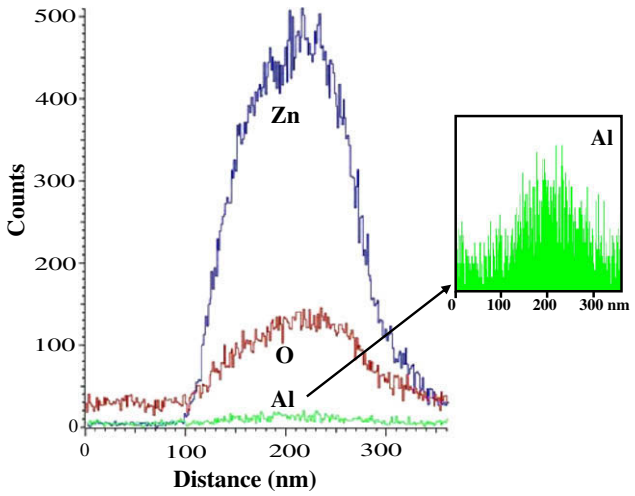

Fig. 2. EDX concentration profiles of Zn, O, and Al along the line drawing in a AZO-coated ZnO nanowire.

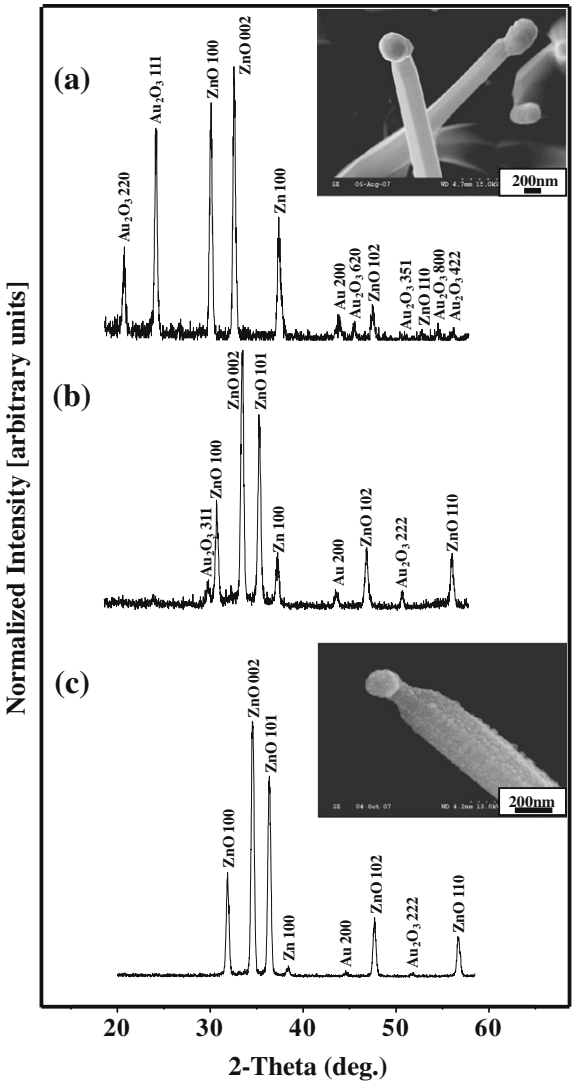

Fig. 3. Normalized XRD patterns of (a) uncoated ZnO nanowires, (b) 10 nm-AZO-sputtered ZnO nanowires, and (c) 20 nm-AZO-sputtered ZnO nanowires (inset: corresponding SEM images exhibiting the tip-part of the nanowires).

TEM image of a region near the surface of a AZO-coated ZnO nanowire. The lattice spacing of the nanowire is approximately 0.26 nm, corresponding to the (0 0 2) fringes of the wurtzite hexagonal ZnO crystal. Although the surface of the nanowire is a little coarse, the corresponding selected area electron diffraction (SAED) pattern suggests that the nanowire is crystalline. Fig. 2 shows the EDX concentration profiles of Zn, O, and Al elements along the line drawing in a typical coated nanowire with a sputter time of 2 min. The EDX profiles clearly confirm the existence of Al, as well as Zn and O.

Fig. 3a shows the XRD pattern of the uncoated ZnO nanowires, whereas Fig. 3b and c exhibit the XRD patterns of the AZO-coated ZnO nanowires sputtered for 1 and 2 min, respectively. The patterns exhibit four crystal phases, i.e., hexagonal ZnO (JCPDS 36-1451), hexagonal Zn (JCPDS 04-0831), cubic Au (JCPDS 04-0784), and orthorhombic Au_2O_3 (JCPDS 43-1039). The ZnO-associated peaks are attributed to the ZnO nanowires. In addition, we surmise that the excessive Zn in the vapor is adsorbed on the solid surface, resulting in Zn peaks [13]. Since the TEM investigation revealed that the nanowires were mainly composed of hexagonal ZnO phase, we surmise that most of the solid Zn would be easily oxidized to ZnO by the residual oxygen [14] and there should exist a relatively small amount of Zn phase in the product. On the other hand, the Au and Au_2O_3 peaks are ascribed to the Au catalysts on the bottom or at the tips of the nanowires. The inset of Fig. 3a shows a selected SEM image of the as-produced ZnO nanowires, which clearly reveals the presence of Au-related particles at their ends. The comparison study in regard to the Au_2O_3(2 2 0), Au_2O_3(1 1 1), and Au(2 0 0) peaks reveals that the relative intensities of those peaks decreased with increasing thickness of the AZO layer. The inset of Fig. 3c shows a selected SEM image of the AZO-coated ZnO nanowires, suggesting that the core ZnO nanowires, including the nanoparticle-comprising tips, have been coated with the AZO layer. Accordingly, we surmise that the Au-associated phases were covered by an AZO layer, resulting in the suppression of the Au- and Au_2O_3-related XRD peaks.

In the present analysis concerning the XRD peak positions, the relatively intense and sharp diffraction peaks corresponding to the (1 0 0) and (0 0 2) indices of ZnO were extracted. Fig. 4 shows the variation of the positions of the ZnO(1 0 0) and ZnO(0 0 2) peaks with the AZO thickness. With regard to the ZnO(1 0 0) orientation, a slight peak shift (0.61°) toward a higher diffraction angle is observed, compared with the core ZnO nanowires (31.25°). Similarly, with regard to the ZnO(0 0 2) orientation, a slight peak shift (0.91°) toward a higher diffraction angle is observed, compared with the core ZnO nanowires (33.69°). It is surmised that Al atoms were incorporated into the ZnO lattice and that they mainly substituted into the Zn sites, resulting in the reduction of the lattice constant [15].

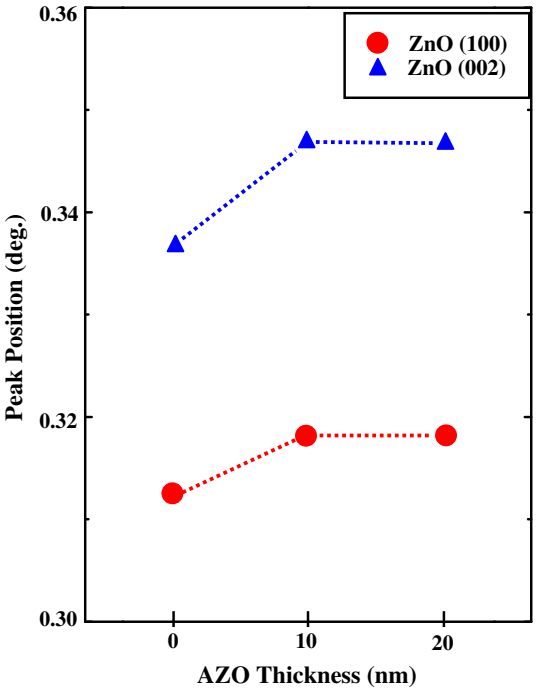

Fig. 4. Variation of peak positions of ZnO(1 0 0) and ZnO(0 0 2) peaks with the AZO thickness.

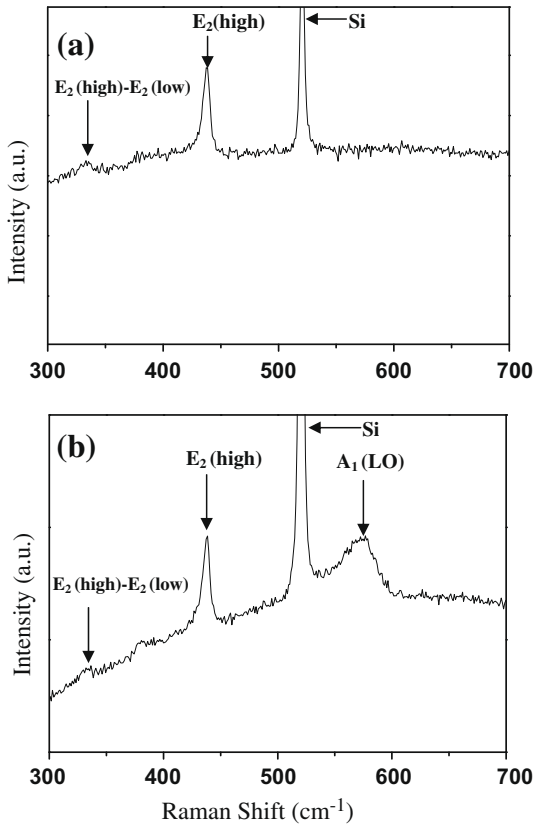

Fig. 5. Room-temperature Raman spectra of (a) uncoated and (b) 20 nm-AZO-sputtered ZnO nanowires.

Fig. 5a shows the room-temperature Raman spectrum of the core ZnO nanowires. The sharp peak at 520 cm^{-1} was identified as the TO phonon mode in the silicon (Si) crystal structure [16], presumably originating from the Si substrates. Besides this peak, the usual modes in ZnO, such as 333 cm^{-1} (E_2(high)-E_2(low) [17–19]) and 437 cm^{-1} (E_2(high) [20–22]), are also observed: On the other hand, in the Raman spectrum of the ZnO nanowires sputtered for 2 min (Fig. 5b), the A_1(LO) mode (573 cm^{-1}) is noticeably observed, whereas it is hardly seen in the spectrum of the uncoated sample (Fig. 5a). The enhancement of the A_1(LO) mode by the Al doping has also been previously reported [17,21,23]. The 573 cm^{-1}-band can be assigned to the electric field-induced (EFI) Raman scattering [21]. It has been reported that a grain boundary depletion layer is formed in the ZnO layers [24]. The doped AZO layers are degenerate and, thus, the concentration difference between the grain boundary and the grain is larger, which leads to the generation of a narrower depletion region. Since the strength of the electric field in the Al-doped grain is higher than that in the undoped one, due to the narrower depletion region, the AZO generates a higher electric field than the undoped ZnO [21]. Accordingly, the A_1(LO) mode via the EFI Raman scattering should be enhanced by the AZO coating.

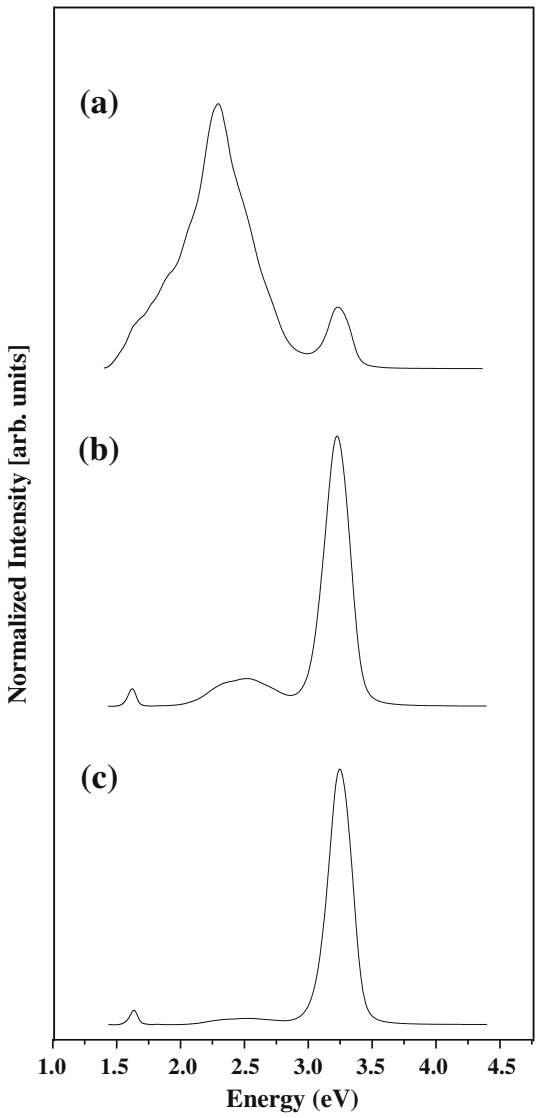

Fig. 6. Normalized PL spectra of the (a) uncoated, (b) 20 nm-AZO-sputtered, and (c) 30 nm-AZO-sputtered ZnO nanowires.

Fig. 6a, b, and c show the PL spectra of the uncoated ZnO nanowires and those AZO-coated with thicknesses of 20 and 30 nm, respectively. The PL emission spectrum shown in Fig. 6a corresponds to the typical emission spectrum of ZnO, which consists of a broad green emission and strong UV emission. Although the AZO-coated ZnO nanowires also exhibit these green and UV emissions, it is noteworthy that the intensity ratio of the UV to green emission was increased by the AZO layer. Also, the ratio was further increased by increasing the thickness of the AZO layer (Fig. 6b and c). It is known that the free energy of formation of Al_2O_3 ($\Delta G_f = -1582.3$ kJ/mol) is much smaller (i.e. negatively larger) than that for ZnO ($\Delta G_f = -320.5$ kJ/mol) [25]. In addition, the bonding strength of Al–O (511 ± 3 kJ/mol) is much higher than that of Zn–O (159 ± 4 kJ/mol) [25]. Accordingly, the Al–O bonds will be easily formed in AZO layer and it is possible that the formation of Al–O bonds in the AZO layers affected the green emission [26]. It is well known that the deep level (green) emission of ZnO is due to the presence of various defects, such as interstitial oxygen and oxygen vacancies. Because Al ions exist in the form of Al^{3+} and Zn ions in the form of Zn^{2+}, when Al element is doped in ZnO, the Al ions will consume the residual O ions and decrease the concentration of interstitial oxygen in the AZO layers. Also, Al is known to reduce the concentration of oxygen vacancies according to the reaction: $Al_2O_3 + V_O^{\bullet\bullet} \rightarrow 2Al_{Zn}^{\bullet} + 3O_O^X$ [27]. Moreover, Kuo et al. postulated that high Al-doping facilitates the nonradiative transition rate, in regard to the localization of the Al impurity states [26]. On the other hand, a weak red emission peak could be observed from the AZO-coated sputtered samples (Fig. 6b and c). It is noteworthy that the red emission shoulder was also found in uncoated sample (Fig. 6a). With the wavelengths of UV and red emissions approximately corresponding to 380 nm and 760 (i.e. $380 * 2$) nm, we surmise that the weak red PL peak is a second-order peak of UV peak. A further systematic study is in progress.

4. Conclusions

In summary, we surrounded ZnO nanowires with AZO shell layers for the first time. We employed a sputtering technique, in which an AZO target was used. The TEM investigation indicates that the shell layers correspond to the hexagonal ZnO phase. The XRD analysis shows that the ZnO diffraction peaks are shifted to higher-angle positions. The EDX spectra reveal that the shell layer comprises Al, as well as Zn and O. The Raman spectra confirm that the addition of Al enhanced the A_1(LO) mode line. The PL analysis reveals that the intensity ratio of the UV to green emission was increased by increasing the thickness of the AZO layer.

Acknowledgement

This work is the outcome of a Manpower Development Program for Energy and Resources supported by the Ministry of Knowledge and Economy (MKE) (No. 37112).

References

[1] J. Hupkes, B. Rech, S. Calnan, O. Kluth, U. Zastrow, H. Siekmann, M. Wuttig, Thin Solid Films 502 (2006) 286.
[2] C.Y. Lee, S.Y. Li, P. Lin, T.Y. Tseng, IEEE Trans. Nanotechnol. 5 (2006) 216.
[3] S.Y. Li, P. Lin, C.Y. Lee, T.Y. Tseng, J. Appl. Phys. 95 (2004) 3711.
[4] S.N. Bai, T.Y. Tseng, Thin Solid Films 515 (2006) 872.
[5] Y. Sun, K.E. Addison, M.R. Ashfold, Nanotechnology 18 (2007) 495601.
[6] J.F. Chang, H.H. Kuo, I.C. Leu, M.H. Hon, Sens. Actuators B 84 (2002) 258.
[7] D. Song, A.G. Aberle, J. Xia, Appl. Surf. Sci. 195 (2002) 291.
[8] R.R. Piticescu, R.M. Piticescu, C.J. Monty, J. Eur. Ceram. Soc. 26 (2006) 2979.
[9] M. Chen, Z.L. Pei, C. Sun, J. Gong, R.F. Huang, L.S. Wen, Mater. Sci. Eng. B 85 (2001) 212.
[10] H.P. He, H.P. Tang, Z.Z. Ye, L.P. Zhu, B.H. Zhao, L. Wang, X.H. Li, Appl. Phys. Lett. 90 (2007) 023104.
[11] H.W. Kim, N.H. Kim, Appl. Phys. A 80 (2005) 537.
[12] K. Shin, K. Prabakar, W.-P. Tai, J.-H. Oh, C. Lee, J. Korean Phys. Soc. 45 (2004) 1288.
[13] X.N. Zhang, C.R. Li, Z. Zhang, Appl. Phys. A 82 (2006) 33.
[14] Y.J. Xing, Z.H. Xi, X.D. Zhang, J.H. Song, R.M. Wang, J. Xu, Z.Q. Xue, D.P. Yu, Appl. Phys. A 80 (2005) 1527.
[15] K.C. Park, D.Y. Ma, K.H. Kim, Thin Solid Films 305 (1997) 201.
[16] M. Hirasawa, T. Orii, T. Seto, Appl. Phys. Lett. 88 (2006) 093119.
[17] A. El Manouni, F.J. Manjón, M. Mollar, B. Marí, R. Gómez, M.C. López, J.R. Ramos-Barrado, Superlatice. Microst. 39 (2006) 185.
[18] S.L. Mensah, V.K. Kayastha, I.N. Ivanov, D.B. Geohegan, Y.K. Yap, Appl. Phys. Lett. 90 (2007) 113108.
[19] A. Umar, B. Karunagaran, E.-K. Suh, Y.B. Hahn, Nanotechnology 17 (2006) 4072–4077.
[20] Y. Tak, D. Park, K. Yong, J. Vac. Sci. Technol. B 24 (2006) 2047.
[21] M. Tzolov, N. Tzenov, D. Dimova-Malinovska, M. Kalitzova, C. Pizzuto, G. Vitali, G. Zollo, I. Ivanov, Thin Solid Films 379 (2000) 28.
[22] K.A. Alim, V.A. Fonoberov, A.A. Balandin, Appl. Phys. Lett. 86 (2005) 053103.
[23] C. Bundersmann, N. Ashkenov, M. Schubert, D. Spenmann, T. Butz, E.M. Kaidashev, M. Lorenz, M. Grundmann, Appl. Phys. Lett. 83 (2003) 1974.
[24] T.L. Tansley, D.F. Neely, Thin Solid Films 121 (1984) 95–107.
[25] D.R. Lide (Ed.), CRC Handbook of Chemistry and Physics, CRC, Boca Raton, FL, 2002.
[26] S.-Y. Kuo, W.-C. Chen, F.-I. Lai, C.-P. Cheng, H.-C. Kuo, S.-C. Wang, W.-F. Hsieh, J. Cryst. Growth 287 (2006) 78.
[27] Y.-G. Wang, N. Ohashi, Y. Wada, I. Sakaguchi, T. Ohgaki, H. Haneda, J. Appl. Phys. 100 (2006) 023524.